Journal of
Materials Chemistry C

Accepted Manuscript

This article can be cited before page numbers have been issued, to do this please use: S. Sandhu, R. Kumar, P. Singh and S. Kumar, *J. Mater. Chem. C*, 2016, DOI: 10.1039/C6TC00655H.

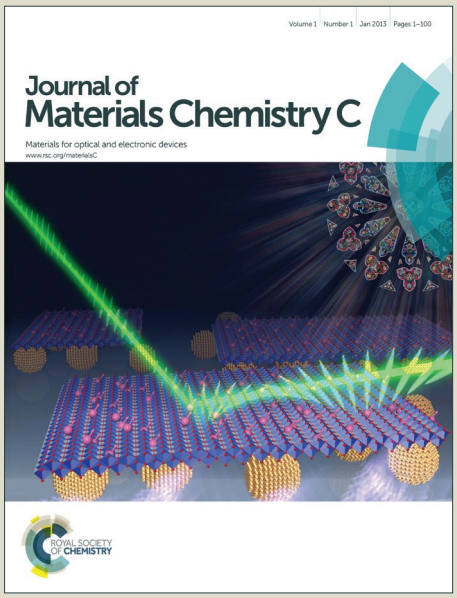

ROYAL SOCIETY OF CHEMISTRY

www.rsc.org/materialsC

View Article Online
DOI: 10.1039/C6TC00655H

Journal Name

ARTICLE

Impact of aggregation on fluorescence sensitivity of molecular probes towards nitroaromatic compounds

Received 00th January 20xx,
Accepted 00th January 20xx

DOI: 10.1039/x0xx00000x

www.rsc.org/

Sana Sandhu[a], Rahul Kumar[a], Prabhpreet Singh[a*], Subodh Kumar[a*]

Abstract: We have designed and synthesized three tripods **TIBP4**, **TIBP8** and **TIBP12** possessing respectively OC_4H_9, OC_8H_{17} and $OC_{12}H_{25}$ alkoxy chains on the biphenyl units and have investigated the effect of chain length on their ease in aggregation and their efficiency in detection of nitroaromatic compounds. Tripods **TIBP8** and **TIBP12** self-assemble to form densely populated nano-spheres (60-100 nm) in water - DMSO (98:2) mixture, as shown by field-emission scanning electron microscopic, transmission electron microscopic and dynamic light scattering studies. **TIBP4** which has shorter *n*-butyl alkyl chains does not undergo aggregation under these conditions. Tripods **TIBP8** and **TIBP12** which remain in self-assembled state in water, reveal amplified fluorescence quenching with PA, 2,4-DNP, TNT and Cl-DNB and are associated with NAC induced dis-aggregation to well dispersed particles. **TIBP8** can detect as low as 10^{-14} M PA and 2,4-DNP in solution and 2.29 x 10^{-20} g/cm^2 (22.9 zeptogm/cm^2) PA by contact mode and is nearly 6000-16000 times more selective towards PA and 2,4-DNP over TNT and Cl-DNB at 20% fluorescence quenching. However, tripod **TIBP12** can detect as low as 10^{-14} M each of PA, 2,4-DNP, TNT and Cl-DNB and can find application as general probe for these NACs. **TIBP4** which remains in moleculalry dissolved state shows poor sensitivity (LOD 1 nM) towards NACs.

Introduction

Improving the sensitivity of a fluorescence probe[1] for the determination of a nitroaromatic compound is one of the major challenge amongst chemists and other scientists working on methods for detection of nitro aromatic explosives. In case of molecularly dissolved probes[2], the stoichiometric interaction of the NAC with fluorescent probe results in modulation of only its fluorescence but other molecules of the probe remain unaffected. As a result, the change in fluorescence intensity is directly proportional to the concentration of NAC and is completed by equimolar or higher concentrations of the NAC.

In an alternative approach, if single molecule of NAC can modulate the fluorescence of large number of fluorophores, the sensitivity of the signal is drastically amplified. To achieve such amplified fluorescence quenching or enhancement, the conjugated polymers[3] have shown tremendous potential but difficulty in their synthesis and structural modifications and poor stability have resulted in many demerits also.

Amongst other approaches, the aggregation of small organic molecules into nano-fibers has shown their tremendous potential in amplifying[4] the fluorescence signal on interaction with NACs. The fluorescent organic aggregates also show exceptionally high sensitivity towards variety of analytes in comparison to molecularly dissolved probes[5]. Such aggregates are easily generated *in situ* by dissolving the concentrated solution of an organic derivative into a non-solvent medium that is a solvent in which the organic derivative has poor solubility. This solvent is usually water and allows the molecules of organic derivative to form well dispersed aggregates in aqueous medium. Such amorphous aggregates allow the single NAC species to remain in the vicinity of large number of fluorophores and thus amplify the modulation of fluorescence through electron, charge or resonance energy transfer processes[6].

We, in our earlier reports[7] have shown that the *p*-terphenyl based molecular probes undergo self-assembly to rod like morphology and these aggregates reveal highly sensitive and selective amplified fluorescence quenching with PA to detect PA as low as 10^{-12} M in solution and 2.29 × 10^{-20} g/cm^2 in contact mode. The biphenyl based tripod[8] remains in molecularly dissolved state, encapsulates PA in its tripodal cavity but could detect only 1 nM PA. This enhanced sensitivity of probe[7] in self-assembled state could be ascribed to increased probability of electron / charge transfer or RET from electron–rich fluorophores to electron-deficient NAC in the aggregate particle in comparison to molecularly dissolved state.

[a]*Department of Chemistry, Guru Nanak Dev University, Amritsar 143005, Punjab, India*

Electronic Supplementary Information (ESI) available: [Spectra of compounds and some photophysical studies are available as supplementary information]. See DOI: 10.1039/x0xx00000x

View Article Online
DOI: 10.1039/C6TC00655H

In literature long alkyl chain bearing imidazolium derivatives are well known to undergo aggregation to form micelle, vesicle or even liquid crystalline state[9]. We envisaged that alkoxy-biphenyl based tripods, depending on the length of alkyl chain, can undergo aggregation in water and such aggregates would show enhanced sensitivity towards PA and other NACs than that observed with probes existing in molecularly dissolved state.

Herein, we have designed three tripods **TIBP4**, **TIBP8** and **TIBP12** which differ from each other only in the length of the alkoxy chain (OC_4H_9, OC_8H_{17} and $OC_{12}H_{25}$) present on the biphenyl unit. We have found that tripods **TIBP8** and **TIBP12** in water (2% DMSO) self-assemble to form densely populated spherical aggregates as observed by FE-SEM, TEM and DLS studies, whereas **TIBP4** does not undergo aggregation and remains in molecularly dissolved state. The aggregates of **TIBP8** and **TIBP12** undergo amplified fluorescence quenching with NACs and can detect as low as 10^{-14} M PA in solution and 2.29 x 10^{-20} g/cm^2 PA by contact mode. The aggregates of **TIBP8** and **TIBP12** are found to be more sensitive to NACs by 10^3 to 10^5 times in comparison to molecular solution of **TIBP4**.

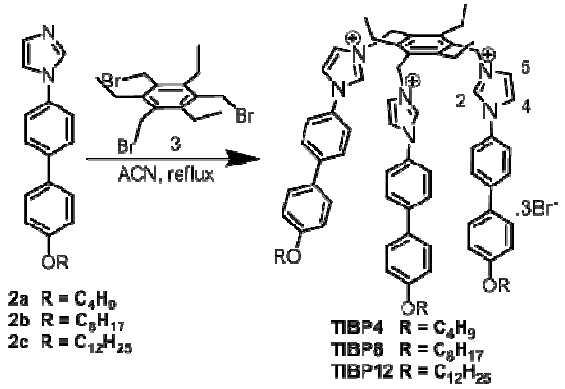

Scheme 1: Synthesis of tripods **TIBP4**, **TIBP8** and **TIBP12**

Synthesis of tripods TIBP4, TIBP8 and TIBP12

The compounds **2a-2c** were synthesized by the procedure reported in literature[9b] (for details see SI) The reaction of **2a** with 1,3,5-tris(bromomethyl)-2,4,6-triethylbenzene (**3**) in acetonitrile at reflux temperature gave white solid in 89 % yield, m.p. 240 °C. The presence of C-2H at δ 9.72, H4-Im at δ 8.43, H5-Im at δ 8.04 (confirmed by NOESY spectrum of **TIBP4**, Figure 1a) along with N-CH_2 singlet at δ 5.64 confirms the formation of **TIBP4**. Similarly, **2b** on refluxing with tribromide (**3**) in acetonitrile gave **TIBP8** in 86.7 % yield, m.p. 248 °C and the reaction of **2c** with tribromide (**3**) gave **TIBP12** in 73.6 % yield, m.p. 251-254 °C. The ^{1}H NMR spectra of these tripods show that H_c and H_d protons in **TIBP12** appear as AB quartet with coupling constant J_1 = 8.5 Hz and Δ = 31 Hz (Figure 1). On moving to **TIBP8** and **TIBP4**, the Δ value is decreased to 21.5 and 12 Hz, respectively. Presumably, the increase in chain length results in aggregation of molecules and increases the compactness[10] of the arms in the tripod **TIBP12**. ^{1}H NMR spectra of **TIBP4**, **TIBP8** and **TIBP12** have been recorded as 5 mM solution in DMSO-d_6.

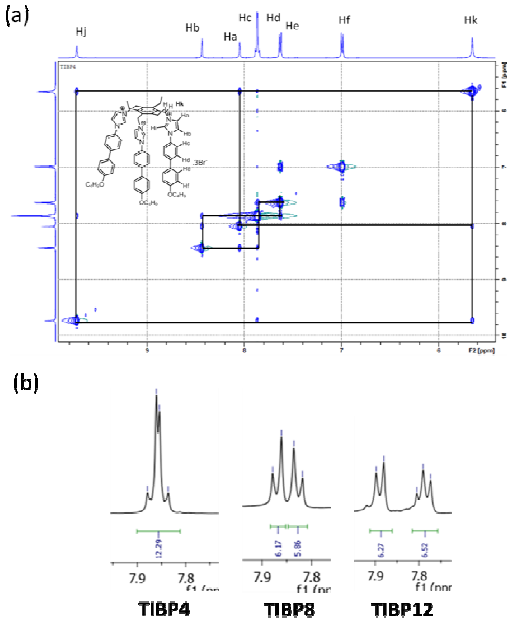

Figure 1: (a) Partial NOESY spectrum of **TIBP4** showing cross peaks and signal assignments; (b) ^{1}H NMR signal of N-phenyl moiety in three tripods

UV-VIS and fluorescence studies of TIBP4, TIBP8 and TIBP12 in binary mixtures

To investigate the aggregation behavior of these tripods, we performed their absorbance and fluorescence measurements in DMSO and DMSO-H_2O binary mixtures with different fractions of water. UV-Vis and fluorescence spectra were recorded at 5 μM concentration. UV-Vis spectrum of **TIBP4** in DMSO exhibits absorption maxima at 292 nm (ε = 77600). On increasing the fraction of water in DMSO, the absorption maxima of **TIBP4** is gradually blue-shifted to 282 nm. The extinction coefficient (ε0 value of the absorption band at 292 nm also gradually decreases and attains minimum value (ε = 53400) in 95% aqueous medium (Figure 2a, SI-1). For all fluorescence studies, 290 nm was used as excitation wavelength. The DMSO solution of **TIBP4** reveals emission maxima at 434 nm, which on increasing the amount of water is gradually red-shifted to 454 nm (Φ = 0.05)[11] and is associated with gradual decrease in fluorescence intensity up to 95% water (Figure 2, SI-1).

UV-Vis spectrum of **TIBP8** in DMSO exhibits absorption maxima at 292 nm (ε = 73400). The solutions of **TIBP8** with increasing fraction of water result in gradual blue-shift of the maxima to 280 nm (ε = 38200) up to 60% water fraction. On further increasing water fraction up to 98%, the absorption maxima and absorption intensity do not show any measurable change. On excitation at 290 nm, DMSO solution of **TIBP8** exhibits emission maximum at 430 nm. On increasing water fraction up to 80%, the emission maxima red-shifts to 448 nm along with gradual decrease in its fluorescence intensity. On

View Article Online
DOI: 10.1039/C6TC00655H

further increasing the fraction of water to 90-98%, the emission maxima is blue shifted to 410 nm (Φ = 0.06)[11] with increase in its intensity (Figure 2b, Figure SI-2). This blue shift of the emission maxima from 448 to 410 nm is ascribed to the aggregation of **TIBP8** molecules in DMSO-H_2O mixtures with > 90% water fraction.

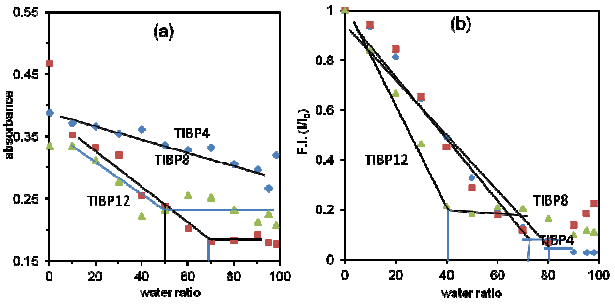

Figure 2: The comparison of change in intensity in UV-Vis and Fluorescence spectra of **TIBP4**, **TIBP8**, and **TIBP12** in binary mixtures with different fractions of water in DMSO

Tripod **TIBP12** in its UV-Vis spectrum elicits the blue shift of the absorption maxima by 12 nm from 290 to 278 nm in solution with 40% water fraction and does not undergo further change in its maxima at higher fractions of water. The recording of fluorescence spectra of **TIBP12** in binary mixtures reveals blue-shift of 16 nm from 428 to 412 nm (Φ = 0.07) associated with significant decrease in the fluorescence intensity in 40% water fraction and points to its aggregation in solutions with > 40 % water fraction (Figure 2, SI-3).

These results clearly show that **TIBP4** undergoes linear decrease in its absorbance for all fractions of water (Figure 2), whereas this linear decrease in absorbance is stopped at 80% and 40% water fractions in case of **TIBP8** and **TIBP12,** respectively. Similarly, in case of fluorescence studies, the fluorescence intensity of **TIBP4** decreases linearly up to 90% water fraction, but **TIBP8** and **TIBP12** undergo decrease in fluorescence up to 80% and 40% water fractions, respectively.

Therefore, **TIBP4** remains in molecularly dissolved state in solutions with all water fractions, **TIBP8** achieves aggregate state in solutions with > 80% water fraction and **TIBP12** starts aggregating in solutions with $\geq$ 40% water fraction.

Aggregation – disaggregation studies by DLS, FE-SEM and TEM techniques

We further investigated the difference in aggregation behaviour of **TIBP8** and **TIBP12** under these conditions using dynamic light scattering (DLS) studies of the solutions and FE-SEM and TEM studies of the thin-films of **TIBP8** and **TIBP12** solutions with and without PA.

DLS measurements of **TIBP8** (1 µM, H_2O-DMSO; 98;2) solution show the formation of aggregates with sizes ranging between 45-105 nm (average size 60 nm) with PDI 0.364 (Figure 3a). FE-SEM and TEM images of thin film obtained from solution of **TIBP8** (1 µM) show the formation of spherical aggregates with ~ 60 nm size (Figure 3b, 3c). Thin films obtained from the solution of **TIBP8** containing 0.1 µM PA, show the presence of well dispersed particles with sizes between 20-60 nm (Figure 3e) which is in agreement with DLS studies (Figure 3d). In the presence of 0.1 equiv. of PA the aggregates are not observed in DLS and FE-SEM studies. The formation of densely populated aggregates of **TIBP8** and their disaggregation to well dispersed and smaller aggregates is also confirmed by TEM studies (Figure 3c, 3f). There are only couple of reports[7,12] where the aggregates of molecular probes undergo dis-aggregation in the presence of nitro aromatic explosives.

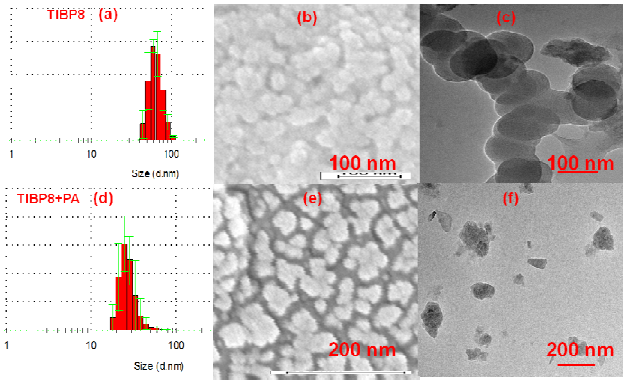

Figure 3: DLS, SEM and TEM images of (a-c) **TIBP8** (10^{-6} M); (d-f) **TIBP8** + PA (10^{-7} M); (water + 2 % DMSO)

Similarly, DLS studies on solution of **TIBP12** (H_2O: DMSO; 98:2)show the formation of aggregates with average size 60 nm, which in the presence of PA undergo disaggregation to average 30 nm size particles (Figure 4a, 4d). FE-SEM and TEM images of the film obtained from the solution of **TIBP12** show the formation of densely populated aggregates (Figure 4b, 4c). However, thin film of the solution of **TIBP12** containing 0.1 equivalent of PA reveals the formation of well dispersed aggregates (Figure 4e, 4f). Therefore, **TIBP8** and **TIBP12** exhibit similar morphological changes in H_2O-DMSO (98:2) solution to form spherical aggregates which in the presence of 0.1 µM PA (0.1 equivalent) undergo disaggregation to form well dispersed particles.

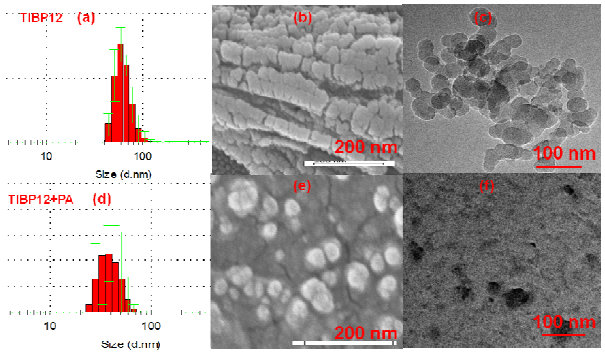

Figure 4: DLS, SEM and TEM images of (a-c) **TIBP12** (10^{-6} M); (d-f) **TIBP12** + PA (10^{-7} M); (water + 2 % DMSO)

View Article Online
DOI: 10.1039/C6TC00655H

UV-Vis and fluorescence studies of TIBP4, TIBP8 and TIBP12 with NACs

In the present study, we have chosen H_2O – DMSO (98:2) as solvent to investigate the interactions of tripods with NACs in the solution. In this solvent medium, **TIBP4** remains in molecularly dissolved state, where as **TIBP8** and **TIBP12** achieve aggregate state. The aromatic compounds investigated are phenol, 2- nitrophenol (2-NP), 4-nitrophenol (4-NP), 2,4-dinitrophenol (2,4-DNP), picric acid (PA), 4-hydroxybiphenyl (4-OHBP); 2-nitrotoluene (2-NT), 2,4-dinitrotoluene (2,4-DNT), dinitrobenzene (DNB), 2-chloronitrobenzene (2-ClNB), trinitrotoluene (TNT); 3-chloronitrobenzene (3-ClNB), 4-chloro-nitrobenzene (4-ClNB), chlorodinitrobenzene (Cl-DNB), 2-nitroaniline (2-NA) and 2,4-dinitroaniline (2,4-DNA).

The UV-Vis absorption spectra of all three tripods show negligible change on addition of 1 equivalent of these aromatic compounds. Therefore, these tripods have only weak interactions with aromatic compounds, in the ground state.

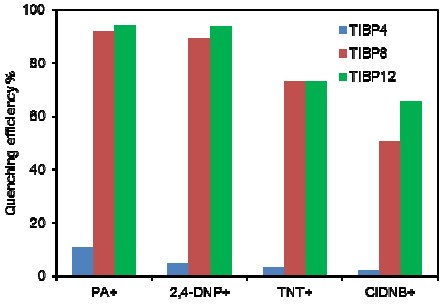

Figure 5: The fluorescence quenching efficiency of the solutions of **TIBP4**, **TIBP8** and **TIBP12** (5 μM) in water-DMSO (98:2) on addition of NACs 0.5 μM

The solutions of **TIBP8** (5 μM) undergo fluorescence quenching by 92, 89, 73 and 51 percent, respectively with 0.5 μM (0.1 equiv.) each of PA, 2,4-DNP, TNT and Cl-DNB (Figure 5). Similarly, the addition of 0.1 equivalent of PA, 2,4-DNP, TNT and Cl-DNB, to the solution of **TIBP12** elicits efficient fluorescence quenching of 94, 93, 73 and 66 %, respectively. The other NACs have insignificant effect on the FI of **TIBP8** and **TIBP12** solutions. Tripod **TIBP4** exhibits only 1-10% fluorescence quenching on addition of 0.5 μM of these NACs. However, **TIBP4** reveals 62, 45, 25 and 14.5 % fluorescence quenching, respectively with 10 μM (2 equiv.) of PA, 2,4-DNP, TNT and Cl-DNB. The other NAC's have insignificant effect on the FI of **TIBP4** solution.

Therefore, **TIBP8** and **TIBP12** derivatives which exist in aggregate state undergo amplified fluorescence quenching in the presence of < 0.1 equiv. of the above discussed four NACs, but **TIBP4** which remains in molecularly dissolved state exhibits smaller quenching of fluorescence even at 2 equiv. of these NACs. This provides the proof of the concept that the probes which attain aggregate state exhibit remarkably enhanced sensitivity towards NACs than those probes which remain in molecularly dissolved state.

Further to find out the limits of detection and Stern-Volmer constant values of these tripod derivatives towards PA, 2,4-DNP, TNT and Cl-DNB, we performed the fluorescence titrations. The FI of **TIBP4** (5 μM, H_2O-DMSO, 98:2) at 454 nm (λ_{ex} 290 nm) gradually decreases on addition of aliquots of NACs and achieves plateau on addition of 30 μM PA, 50 μM 2,4-DNP, 70 μM TNT and 200 μM Cl-DNB (Figures 6, SI-4). At lower concentrations of NACs, the fluorescence quenching follows Stern-Volmer equation, $I_o/I = 1 + K_{SV}[Q]$. The Stern-Volmer constant for PA (6.25×10^5 M^{-1}) is larger in comparison to K_{SV} values for 2,4-DNP (5.03×10^4 M^{-1}), TNT (1.84×10^4 M^{-1}) and Cl-DNB (1.35×10^4 M^{-1}). The lowest detection limits are found to be 2.5×10^{-8} M for PA, 5×10^{-7} M for 2,4-DNP, 1×10^{-6} M for TNT and Cl-DNB. **TIBP4** shows fluorescence quenching efficiency in the order PA > 2,4-DNP > TNT > Cl-DNB.

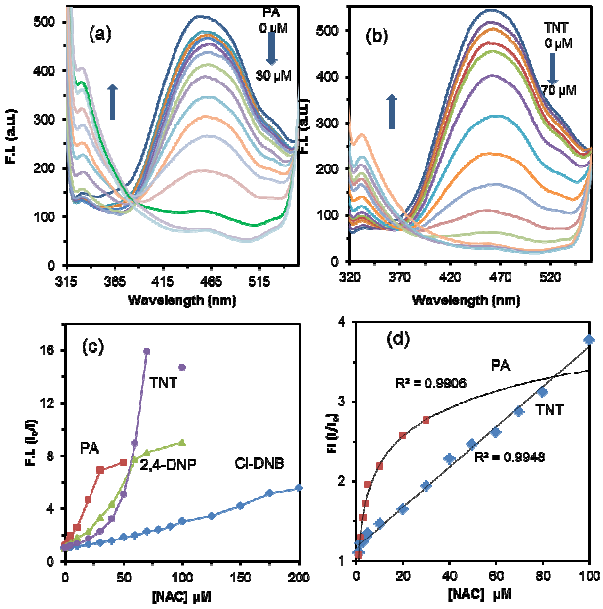

Figure 6: Fluorescence spectra of **TIBP4** , on gradual addition of (a) picric acid; (b) TNT (c) Plot of I_o/I vs [NAC] of fluorescence titration of **TIBP4** with PA, 2,4-DNP, TNT and Cl-DNB; (d) Plot of FI (I/I_o) vs [PA] / [TNT] at concentrations > 1 μM showing fluorescence enhancement at 335 nm

Characteristically, **TIBP4** forms fluorescent complexes with maxima centered at 340 nm and 332 nm at ≥ 1 equivalent concentrations of PA and TNT. These complexes exhibit linear change in its fluorescence intensity at ~ 335 nm between 2-30 μM of PA and 10 μM – 100 μM of TNT with maximum fluorescence intensity enhancement by 170 and 280%, respectively (Figure 6d). The formation of fluorescent complexes by NACs is relatively un-known phenomenon.

Tripods **TIBP8** and **TIBP12**, which exists in aggregate state in H_2O (2% DMSO) reveal more efficient fluorescence quenching with PA, 2,4-DNP, TNT and Cl-DNB at 410 nm (Figure 7, SI-5, SI-6). The plots of I/I_o vs [NAC] show non-linear change and do not follow Stern-Volmer equation $I_o/I = 1 + K_{SV}[Q]$. Therefore, K_{SV} values of **TIBP8** and **TIBP12** for the detection of PA, 2,4-DNP, TNT and Cl-DNB have been calculated by exponential equation $I/I_o = Ae^{K_{SV}[Q]} + B$ using

View Article Online
DOI: 10.1039/C6TC00655H

origin software (Figure 7). K_{SV} values for **TIBP8** and **TIBP12** have been found in the order 10^{11} to 10^{10} for PA, 2,4-DNP and TNT which are higher by the order of 3-5 in comparison to those determined for **TIBP4** (Table SI-1). Such high K_{sv} values are well known for the non-conjugated polymers or aggregates[13]. For determining the selectivity of **TIBP8** towards these NACs, the concentrations of these NACs at 20% fluorescence quenching has been determined (Table 1), which is found to be $5x10^{-12}$ M (PA), $5x10^{-11}$ M (2,4-DNP), $3x10^{-8}$ M (TNT) and $8x10^{-8}$ M (Cl-DNB). Under these conditions, **TIBP8** is selective towards PA by 10, 6000, 16000 times in comparison to 2,4-DNP, TNT and Cl-DNB. The detection limits $(3\sigma/m)$[14] for PA, 2,4-DNP, TNT and Cl-DNB are calculated to be 1 x 10^{-14} M, 1 x 10^{-14} M, 5 x10^{-14} M and 5 x10^{-12} M, respectively.

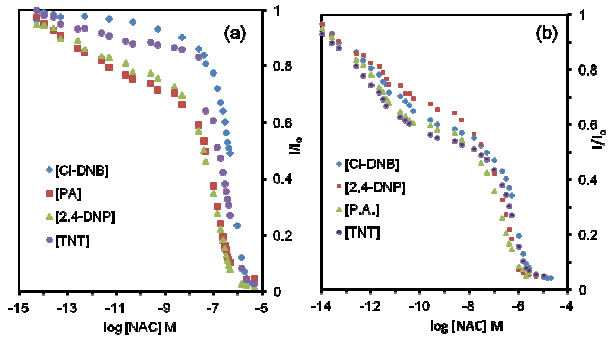

Figure 7: Plot of I/I_o vs log [NAC] M of fluorescence titration against PA, 2,4-DNP, TNT and Cl-DNB **(a) TIBP8 (b) TIBP12**

Table 1: [NAC] at which 20 % of fluorescence quenching of probe

Probe	PA	2,4-DNP	TNT	Cl-DNB
TIBP4	1x10^{-6} M	3 x10^{-6} M	8 x10^{-6} M	18 x10^{-6} M
TIBP8	5x10^{-12} M	5x10^{-11} M	3x10^{-8} M	8x10^{-8} M
TIBP12	10^{-12} M	3x10^{-12} M	5x10^{-13} M	2x10^{-12} M

Tripod **TIBP12** undergoes > 50% fluorescence quenching with 0.1 equivalent of PA, 2,4-DNP, TNT and Cl-DNB which implies 50% fluorescence of **TIBP12** molecules is quenched by 10% **PA** molecules. **TIBP12** elicits poor selectivity towards these NACs. In fact, **TIBP12** can determine PA, 2,4-DNP, TNT and Cl-DNB with equal ease. In comparison with **TIBP8**, the sensitivity of **TIBP12** towards TNT and Cl-DNB has remarkably improved.

Mechanism of interaction of TIBP4, TIBP8 and TIBP12 with NACs

In order to rationalize the interaction of **TIBP4** with PA, ^{1}H NMR spectrum of **TIBP4** before and after addition of PA was recorded in DMSO-d_6-water (7:3) at 5 mM concentration. In ^{1}H NMR spectrum of the solution of 1:1 mixture of **TIBP4** and PA, the up-field shift of 2H singlet of PA from δ 8.62 (in ^{1}H NMR spectrum of PA) to 8.39 (Δ δ = 0.23) points to the encapsulation of PA in the cavity of **TIBP4** (Figure SI-7). However, this up-field shift of PA protons is significantly lower than ~ 0.8 ppm up-field shift in case of earlier reported biphenyl[8] based tripod. ^{1}H NMR spectra of **TIBP8** and **TIBP12** in DMSO-d_6-water (1:1) show broad peaks due to the aggregation of these molecules at high concentrations. The addition of PA to these solutions resulted in precipitation.

The overlap of UV-Vis spectra of NAC with fluorescence spectrum of fluorophore points to the presence of RET process in their interaction. Fluorescence spectra of **TIBP8** and **TIBP12** show nearly 50% overlap with absorption spectra of PA and 2,4-DNP but poor spectral overlap with TNT and Cl-DNB molecules (Figure SI-8). Therefore, **TIBP8** and **TIBP12** might follow, at least partly, RET process for efficient fluorescence quenching with these NACs. The proximity of fluorophores in the aggregate state with NAC molecules and fast electron transfer from ground state of fluorophore to the NAC further increases the efficiency of fluorescence quenching. The fluorescence spectrum of **TIBP4** shows poor overlap with the absorption spectrum of PA and efficiency of RET process is decreased. The lesser proximity of the fluorophores with an NAC molecule due to its molecularly dissolved state also attributes to its lower sensitivity towards NACs.

Contact mode method for detection of PA

Paper strips coated with **TIBP8** reveal observable fluorescence change on addition of 10 µl solutions of 10^{-17} M - 10^{-9} M PA and at higher concentrations only black area is observed (Figure 8). 10 µl of 10^{-17} M solution of PA is equivalent to 2.29 x 10^{-20} g PA. The steady-state fluorescence spectra of these paper strips were recorded. The plot of I_o/I vs log [NAC] shows the linear increase in fluorescence quenching efficiency on moving from 10^{-17}-10^{-9} M PA (Figure 9). However, paper strips coated with **TIBP4** show measurable change with PA in concentration range 10^{-13} to 10^{-7} M both under UV light and steady state fluorescence measurements. In case of **TIBP12** coated paper strips, on addition of 10 µl

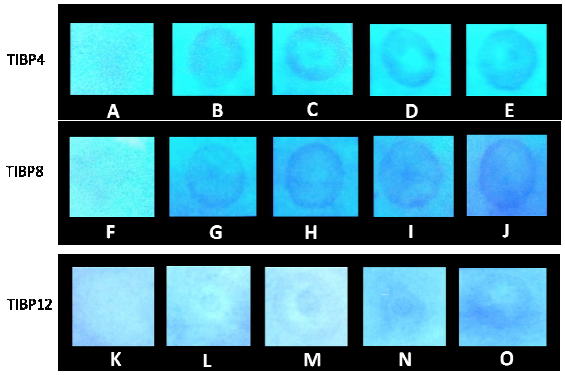

Figure 8: Photographs of fluorescence quenching (under 365 nm UV light) of tripod coated paper strips and 10 µl of different concentrations of PA.(A-E) **TIBP4** (A) Paper strip with a drop of water; (B) 10^{-13} M PA; (C) 10^{-11} M PA; (D) 10^{-9} M PA; (E) 10^{-7} M PA; (F-J) **TIBP8** (F) Paper strip with a drop of water; (G) 10^{-17} M PA; (H) 10^{-15} M PA; (I) 10^{-13}M PA; (J) 10^{-11} M PA. (K-O) **TIBP12** (K) Paper strip with a drop of water; (L) 10^{-17} M PA; (M) 10^{-15} M PA; (N) 10^{-13}M PA; (O) 10^{-11} M PA

View Article Online
DOI: 10.1039/C6TC00655H

solution of water of PA solution, it took > 4 minutes for the drop to be absorbed by the paper strip and exhibits some significant change in fluorescence intensity only on addition of 10^{-13} M or higher concentrations of PA. Probably, **TIBP12** coated paper strips are too hydrophobic to allow the aqueous droplet to absorb on it.

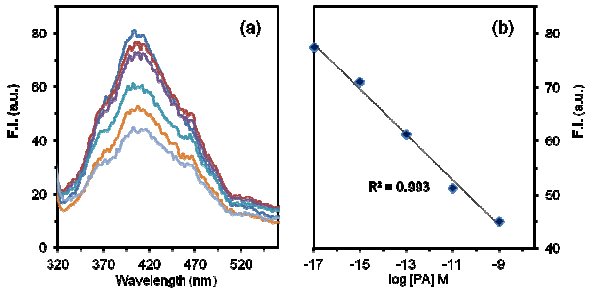

Figure 9: (a) Front surface steady-state fluorescence quenching of **TIBP8** with PA. 10 µl of 10^{-17}-10^{-9} M concentrations of PA added. (b) Plot of fluorescence intensity of **TIBP8** vs log [PA] M

For further exploring the applicability of **TIBP8** and **TIBP12** for detection of PA vapour, thin films of **TIBP8** and **TIBP12** (20 µL, 20 µM) were fabricated through drop cast method on pre-cleaned glass plate surface and were allowed to dry in incubator at 25°C. The fluorescence intensity of the thin-films decreased gradually on exposure to PA vapour at regular intervals of time. In case of film of **TIBP8**, 18 % fluorescence quenching was observed on exposure of 30 seconds to saturated vapour pressure of PA, whereas **TIBP12** underwent only 4.7 % fluorescence quenching under similar conditions. The overall fluorescence quenching efficiency was found to be 55 % in case of **TIBP8** and 40 % in case of **TIBP12**. In both the cases, plateau was achieved after 300 secs of exposure (Figure SI-9). These results are in consonance with higher sensitivity of **TBP12** over **TIBP8** as observed above.

*CONCLUSION*S

In summary, tripods **TIBP8** and **TIBP12** self-assemble in aqueous medium and exhibit amplified fluorescence quenching with PA, 2,4-DNP, TNT and Cl-DNB. **TIBP4** under these conditions remains in molecularly dissolved state and shows poor sensitivity towards PA and other NACs. These results unambiguously highlight the significance of self-assembled materials in developing highly sensitive probes for NACs. **TIBP8** exhibits 20% fluorescence quenching with PA at 6000-16000 times lower concentration than that observed with TNT and Cl-DNB. **TIBP8** can detect as low as 10^{-14} M PA in solution and 2.29 x 10^{-20} g/cm^2 PA by contact mode. However, **TIBP12** is equally sensitive towards all four NACs and can detect as low as 10^{-14} M each of PA, 2,4-DNP, TNT and Cl-DNB and can find application as general sensor for NACs. The increased hydrophobic character of **TIBP12** restricts its applications in contact mode.

Experimental Section

For general experimental information and instrumentation see ref 7 and SI.

Synthesis of tripods TIBP4/ TIBP8/ TIBP12: The solution of 1,3,5-tris(bromomethyl)-2,4,6-triethylbenzene (0.18 mmol, 79.38 mg) and **2a** (0.54 mmol, 218 mg) in acetonitrile was refluxed for 40 h. The solid separated during the course of the reaction was filtered to get **TIBP4** as white solid. The solid was found to be pure. Similar reactions of **2b** and **2c** gave **TIBP8** and **TIBP12**, respectively.

TIBP4: Yield 89 %; m.p. 240°C. **^{1}H NMR** (500 MHz, DMSO-d_6) : δ 0.96 (t, 9H, J = 7.5 Hz, 3 x CH_3), 0.99 (bs, 9H, 3 x CH_3), 1.43-1.50 (m, 6H, 3 x CH_2), 1.73 (quintet, 6H, J = 6.5 Hz, 3 x CH_2), 2.82 (d, 6H, J = 6.5 Hz, 3 x CH_2), 4.01 (t, 6H, J = 6.5 Hz, 3 x CH_2), 5.64 (bs, 6H, 3 x CH_2), 6.98 (d, 6H, J = 9 Hz, ArH), 7.62 (d, 6H, J = 8.5 Hz, ArH), 7.86 (q, 12H, ArH), 8.04 (s, 3H, Im-H), 8.43 (s, 3H, Im-H), 9.72 (s, 3H, Im-C2H); **^{13}C NMR** (500 MHz, DMSO-d_6): δ 14.2, 15.8, 19.2, 31.2, 67.8, 115.5, 121.9, 123.2, 123.9, 127.7, 128.4, 128.8, 130.8, 133.6, 135.3, 141.6, 148.4, 159.4. **HRMS-ESI :** calculated for $C_{72}H_{81}Br_3N_6O_3$, m/z 578.2777 $[M\text{-}2Br^-]^{2+}$, 354.5404 $[M\text{-}3Br^-]^{3+}$; found 578.2758 $[M\text{-}2Br^-]^{2+}$, 354.2116 $[M\text{-}3Br^-]^{3+}$.

TIBP8: Yield 86.7 %, m.p. 248°C; **^{1}H NMR** (500 MHz, DMSO-d_6) **:** δ 0.87 (t, 9H, J = 7 Hz, 3 x CH_3), 1.00 (bs, 9H, 3 x CH_3), 1.27-1.32 (m, 30H, CH_2), 1.40-1.46 (m, 6H, 3 x CH_2), 1.74 (quintet, 6H, J = 6.5 Hz, 3x CH_2), 2.81 (bs, 6H, 3 x CH_2), 3.99 (t, 6H, J = 6.5 Hz, 3 x CH_2), 5.64 (bs, 6H, 3 x CH_2), 6.96 (d, 6H, J = 8.5 Hz, ArH), 7.60 (d, 6H, J = 9 Hz, ArH), 7.83 (d, 6H, J = 9 Hz, ArH), 7.87 (d, 6H, J = 8.5 Hz, ArH), 8.07 (s, 3H, Im-H), 8.43 (s, 3H, Im-H), 9.68 (s, 3H, Im-C2H); **^{13}C NMR** (500 MHz, DMSO-d_6): δ 14.8, 16.0, 23.0, 26.4, 29.6, 29.6, 29.7, 32.1, 48.3, 68.5, 115.9, 122.3, 123.7, 124.5, 128.1, 128.8, 129.2, 131.2, 134.2, 135.8, 142.0, 159.8. **HRMS-ESI :** calculated for $C_{83}H_{103}Br_3N_6O_3$, m/z 655.3637 $[M\text{-}2Br^-]^{2+}$, 410.6030 $[M\text{-}3Br^-]^{3+}$; found 654.8922 $[M\text{-}2Br^-]^{2+}$, 410.6436 $[M\text{-}3Br^-]^{3+}$.

TIBP12: Yield 73.6 %, m.p. 251-254°C; **^{1}H NMR** (500 MHz, DMSO-d_6) **:** δ 0.84 (t, 9H, J = 7 Hz, 3 x CH_3), 1.24-1.33 (m, 60H, CH_2), 1.40-1.44 (m, 6H, 3 x CH_2), 1.73 (t, 9H, J = 7.5 Hz, 3 x CH_3), 3.97 (t, 6H, J = 6.5 Hz, CH_2), 5.65 (s, 6H, 3 x CH_2), 6.92 (d, 6H, J = 8.5 Hz, ArH), 7.56 (d, 6H, J = 8.5 Hz, ArH), 7.78 (d, 6H, J = 8.5 Hz, ArH), 7.89 (d, 6H, J = 8.5 Hz, ArH), 8.13 (s, 3H, Im-H), 8.42 (s, 3H, Im-H), 9.69 (s, 3H, Im-C2H); **^{13}C NMR** (500 MHz, DMSO-d_6) : δ 14.4, 15.9, 22.6, 26.0, 29.2, 29.2, 29.4, 29.5, 29.5, 31.8, 47.9, 68.1, 115.4, 121.8, 123.3, 124.2, 127.5, 128.3, 128.8, 130.8, 133.6, 135.2, 141.4, 148.5, 159.4; **HRMS-ESI :** calculated for $C_{96}H_{131}Br_3N_6O_3$, m/z 747.9750 $[M\text{-}2Br^-]^{2+}$, 472.3438 $[M\text{-}3Br^-]^{3+}$; found 747.9715 $[M\text{-}2Br^-]^{2+}$, 472.3411 $[M\text{-}3Br^-]^{3+}$.

UV-Vis and Fluorescence Titrations

Stock solutions of **TIBP4, TIBP8 and TIBP12** (1 mM) were prepared in DMSO. For experiments with **TIBP4, TIBP8 and TIBP12**, we have taken 3 ml of the solution that contains 15 µL stock solution in DMSO, 45 µL of DMSO and 2.94 ml of water in cuvette. Typically, aliquots of freshly prepared standard solutions (10^{-1} M) of NACs in DMSO were used to record UV-Vis and fluorescence spectra.

View Article Online
DOI: 10.1039/C6TC00655H

Detection limit[14]

The detection limit was calculated based on the fluorescence titration. To determine the S/N ratio, the emission intensity of tripod (5 μM) was measured 5 times and the standard deviation of blank measurements was determined. The detection limit was then calculated with the equation:

Detection limit = 3σbi/m

Where, σbi is the standard deviation of blank measurements; m is the slope between intensity versus sample concentration. The detection limit was measured to be 1 nM at S/N = 3.

Acknowledgements

This work was supported by Department of Science and Technology, New Delhi (SR/S1/OC-75/2012). We thank UGC for UPE programme to the university and CAS status to the department and DST for FIST programme. SS and RK acknowledge DST and UGC for fellowships.

References

1 (a) Y. Salinas, R. Martinez-Manez, M. D. Marcos, F. Sancenon, A. M. Castero, M. Parra and S. Gil, *Chem. Soc. Rev.*, 2012, **41**, 1261-1296; (b) M. E. Germain and M. J. Knapp, *Chem. Soc. Rev.*, 2009, **38**, 2543-2555; (c) G. V. Zyryanov, D. S. Kopchuk, I. S. Kovalev, E. V. Nosov, V. L. Rusinov and O. N. Chupakhin, *Russ. Chem. Rev.*, 2014, **83**, 783-819; (d) S. Shanmugaraju and P. S. Mukherjee, *Chem. Eur. J.,* 2015, 21, 6656-6666; (e) S. Shanmugaraju and P. S. Mukherjee, *Chem. Commun.*, 2015, **51**, 16014-16032; (f) K. K. Kartha, A. Sandeep, V. K. Praveen and A. Ajayaghosh, *Chem. Rec.* 2015, **15**, 252-265.

2 (a) S. Lee, K. K. Y. Yuen, K. A. Jolliffe and J. Yoon, *Chem. Soc. Rev.,* 2015, **44**, 1749-1762; (b) K. Chen, Q. Shu and M. Schmittel, *Chem. Soc. Rev.,* 2015, **44**, 136-160; (c) M. E. Moragues, R. Martinez-Manez and Felix Sancenon, *Chem. Soc. Rev.,* 2011, **40**, 2593–2643; (d) K. Kaur, R. Saini, A. Kumar, V. Luxami, N. Kaur, P. Singh and S. Kumar, *Coord. Chem. Rev.,* 2012, **256**, 1992–2028; (e) T. D. Ashton, K. A. Jolliffe and F. M. Pfeffer, *Chem. Soc. Rev.,* 2015, **44**, 4547-4595. (f) M. Wenzel, J. R. Hiscock and P. A. Gale, *Chem. Soc. Rev.*, 2012, **41**, 480–520.

3 (a) S. W. Thomas, G. D. Joly, and T. M. Swager, *Chem. Rev.* 2007, **107**, 1339-1386; (b) S. J. Toal and W. C. Trogler, *J. Mater. Chem.*, 2006, **16**, 2871-288; (c) H. Sohn, M. J. Sailor, D. Magde, W. C. Trogler, *J. Am. Chem. Soc.*, 2003, **125**, 3821-3830; (d) A. Rose, Z. Zhu, C. F. Madigan, T. M. Swager, V. Bulovi, Nature 2005, **434**, 876-879; (e) J. S. Yang, T. M. Swager, *J. Am. Chem. Soc.,* 1998, **120**, 5321-5322; (f) S. Rochat and T. M. Swager, *ACS Appl. Mater. Interfaces*, 2013, 5, 4488–4502.

4 (a) Y. Wang, A. La, Y. Ding, Y. Liu, Y. Lei, *Adv. Funct. Mater.,* 2012, **22**, 3547-3555; (b) C. Zhang, Y. Che, X. Yang, B. R. Bunes, L. Zang, *Chem. Commun.,* 2010, **46**, 5560-5562; (c) K. Balakrishnan, A. Datar, W. Zhang, X. Yang, T. Naddo, J. Huang, J. Zuo, M. Yen, J. S. Moore, L. Zang, *J. Am. Chem. Soc.,* 2006, **128**, 6576-6577; (d) T. Naddo, Y. Che, W. Zhang, K. Balakrishnan, X. Yang, M. Yen, J. Zhao, J. S. Moore, L. Zang, *J. Am. Chem. Soc.,* 2007**, 129**, 6978-6979; (e) K. K. Kartha, S. S. Babu, S. Srinivasan, A. Ajayaghosh, *J. Am. Chem. Soc.,* 2012, **134**, 4834-4841.

5 (a) J. Suk, Z. Wu, L. Wang and A. J. Bard, *J. Am. Chem. Soc.,* 2011, **133**, 14675−14685; (b) Q. Zhao, K. Li, S. Chen, A. Qin, D. Ding, S. Zhang, Y. Liu, B. Liu, J. Z. Sun and B. Z. Tang, *J. Mater. Chem.,* 2012, **22**, 15128-15135; (c) J. Wang, X. Xu, L. Shi, and L. Li, *ACS Appl. Mater. Interfaces.,* 2013, **5**, 3392-3400; (d) A. Singh, T. Raj, T. Aree and N. Singh, *Inorg. Chem.,* 2013, **52**, 13830–13832; (e) K. Tayade, A. Kaurb, S. Tetgurea, G. K. Chaitanya, N. Singh and A. Kuwar, *Analytica Chimica Acta.,* 2014, **852**, 196-202.

6 X. Sun, Y. Wang and Y. Lei, *Chem. Soc. Rev*., 2015, **44**, 8019-8061.

7 S. Sandhu, R. Kumar, P. Singh, A. Mahajan, M. Kaur and S. Kumar, *ACS Appl. Mater. Interfaces*, 2015, **7**, 10491–10500.

8 R. Kumar, S. Sandhu, P. Singh, G. Hundal, M. S. Hundal and S. Kumar, *Asian J. Org. Chem.*, 2014, **3**, 805–813.

9 (a) A. A. Fernandez, L. T. Haan and Paul H. J. Kouwer, *J. Mater. Chem. A,* 2013, **1**, 354-357; (b) P. H. J. Kouwer and T. M. Swager, *J. Am. Chem. Soc.,* 2007, **129**, 14042–14052; (c) J. Cai and J. L. Sessler, *Chem. Soc. Rev.,* 2014, **43**, 6198-6213; (d) B. Xin and J. Hao, *Chem. Soc. Rev.,* 2014, **43**, 7171-7187; (e) T. Welton, *Chem. Rev.,* 1999, **99**, 2071–2084; (f) C. C. Tzschucke, C. Markert, W. Bannwarth, S. Roller, A. Hebel and R. Haag, *Angew. Chem., Int. Ed.,* 2002, **41**, 3964-4000; (g) M. Trilla, R. Pleixats,T. Parella, C. Blanc, P. Dieudonne, Y. Guari and M. W. C. Man, *Langmuir,* 2008, **24**, 259–265; (h) R. Rondla, J. C. Y. Lin, C. T. Yang and I. J. B. Lin, *Langmuir,* 2013, **29**, 11779–11785; (i) X. Wang, M. Sternberg, F. T. U. Kohler, B. U. Melcher, P. Wasserscheid and K. Meyer, *RSC Adv.,* 2014, **4**, 12476-12481.

10 F. D'Anna, S. Marullo, G. Lazzara, P. Vitale, and R. Noto, *Chem. Eur. J.,* 2015, **21**, 14780–14790.

11 J. N. Demas and G. A. Grosby, *J. Phys. Chem*., 1971, **75**, 991–1024.

12 S. K. Kim, J. M. Lim, T. Pradhan, H. S. Jung, V. M. Lynch, J. S. Kim, D. Kim and J. L. Sessler, *J. Am. Chem. Soc*., 2014, **136**, 495–505.

13 (a) V. Balzani, P. Ceroni, S. Gestermann, C. Kauffmann, M. Gorka and F. Vogtle. *Chem. Commun.,* 2000, 853–854; (b) Y. Sun, Z. Chen, E. Puodziukynaite, D. M. Jenkins, J. R. Reynolds and K. S. Schanze, *Macromolecules,* 2012, **45**, 2632–2642; (c) D. Ghosh and N. Chattopadhyay, *Journal of Luminescence*, 2015, **160**, 223-232; (d) Q. Xu, J. Liu, Z. He and S. Yang, *Chem. Commun.,* 2010, **46**, 8800-8802; (e) J. Chen, Y. Wang, W. Li, H. Zhou, Y. Li and C. Yu, *Anal. Chem.,* 2014, **86**, 9866–9872.

14 J. Mokac, A. M. Bond, S. Mitchell and G. Scollary, *Pure Appl. Chem*., 1997, **69**, 297-328.

View Article Online
DOI: 10.1039/C6TC00655H

Impact of aggregation on fluorescence sensitivity of molecular probes towards nitroaromatic compounds

Sana Sandhu, Rahul Kumar, Prabhpreet Singh, Subodh Kumar

Aggregation of the molecular probe increases its fluorescence sensitivity towards nitroaromatic explosives by the order of 10^3 to 10^5 times.